Computers and Concrete, Vol. 7, No. 3 (2010) 203-220
DOI: http://dx.doi.org/10.12989/cac.2010.7.3.203

Numerical analysis of under-designed reinforced concrete beam-column joints under cyclic loading

Saptarshi Sasmal[1]*, Balthasar Novák[2] and K. Ramanjaneyulu[3]

[1]*Institute for Lightweight Structures and Conceptual Design (ILEK), Universitaet Stuttgart, Germany and Scientist, Structural Engineering Research Centre (SERC), Council for Scientific and Industrial Research (CSIR), Taramani, Chennai-600113, India*
[2]*Institute for Lightweight Structures and Conceptual Design (ILEK), Universitaet Stuttgart, Germany*
[3]*Structural Engineering Research Centre (SERC), CSIR, Taramani, Chennai-600113, India*

(Received September 14, 2009, Accepted March 10, 2010)

Abstract. In the present study, exterior beam-column sub-assemblage from a regular reinforced concrete (RC) building has been considered. Two different types of beam-column sub-assemblages from existing RC building have been considered, i.e., gravity load designed ('GLD'), and seismically designed but without any ductile detailing ('NonDuctile'). Hence, both the cases represent the under-designed structure at different time frame span before the introduction of ductile detailing. For designing 'NonDuctile' structure, Eurocode and Indian Standard were considered. Non-linear finite element (FE) program has been employed for analysing the sub-assemblages under cyclic loading. FE models were developed using quadratic concrete brick elements with embedded truss elements to represent reinforcements. It has been found that the results obtained from the numerical analysis are well corroborated with that of experimental results. Using the validated numerical models, it was proposed to correlate the energy dissipation from numerical analysis to that from experimental analysis. Numerical models would be helpful in practice to evaluate the seismic performance of the critical sub-assemblages prior to design decisions. Further, using the numerical studies, performance of the sub-assemblages with variation of axial load ratios (ratio is defined by applied axial load divided by axial strength) has been studied since many researchers have brought out inconsistent observations on role of axial load in changing strength and energy dissipation under cyclic load.

Keywords: beam-column sub-assemblage; axial load effect; energy dissipation; material modelling, plasticity; fracture energy; numerical analysis; cyclic loading.

1. Introduction

A large number of the existing structures throughout the world were constructed before 1970s' when only gravity load was considered for design. Even, in substantial number of newly built structures hardly any ductile codal provision is followed and gravity load design ('GLD') concept is still practiced. On the other hand, after 1970s' and before introduction of ductile detailing and capacity design concept, though earthquake forces were considered in designing the important structures, but devastating effect from lack of ductile detailing in those structures has been witnessed from previous earthquakes. Generally, a three phase approach is followed to describe a

* Corresponding author, Research Scholar, E-mail: sasmalsap@gmail.com, saptarshi@sercm.org

structure under seismic loading, i.e., (i) the structure must have adequate lateral stiffness to control the inter-story drifts such that no damage would occur to non-structural elements during minor but frequently occurring earthquakes, (ii) during moderate earthquakes, some damage to non-structural elements is permitted, but the structural element must have adequate strength to remain elastic so that no damage would occur, and (iii) during rare and strong earthquakes, the structure must be ductile enough to prevent collapse by aiming for repairable damage which would ascertain economic feasibility. Hence, it is utmost important to evaluate the performance of the existing structures/components under reverse cyclic loading and to find out a realistic model (geometric- and material- models, bond-slip, support condition, etc. along with computational issues) for further parametric studies. It has also been proved that the beam-column joints are the single most critical component of RC structures under seismic loading and their performance under seismic loading needs to be thoroughly understood (Pampanin *et al*. 2003, Zhou 2009). Beside experimental investigations, few studies have also been reported on performance evaluation of existing structure/ components by employing analytical- and numerical-means.

Non-linear finite element (FE) analysis of beam-column joint under monotonic loading has been reported in Hegger *et al*. (2003, 2004). To study the effect of several design parameters (effects of axial load in column, beam to column depth etc.) on seismic behaviour of beam-wide column joints, numerical models were proposed in Li *et al*. (2003) and cyclic load analysis was performed. Using a non-linear FE analysis, Sritharan *et al*. (2000) have shown that how the analysis of reinforced concrete structures subjected to seismic actions can be improved by using nonlinear spring elements to model bond-slip. Fischinger *et al*. (2004) proposed a special vertical-line macro-element in numerical analysis for predicting seismic response of RC walls subjected to a series of consequent earthquakes. Marefat *et al*. (2005) investigated the hysteretic response of sub-standard RC columns under reverse cyclic loading and the responses were compared with the columns designed based on ACI-318. Finally, a relationship has been established between the length of plastic hinge and imposed displacement amplitude.

From the review, it has been found that though few attempts have been made to explore the

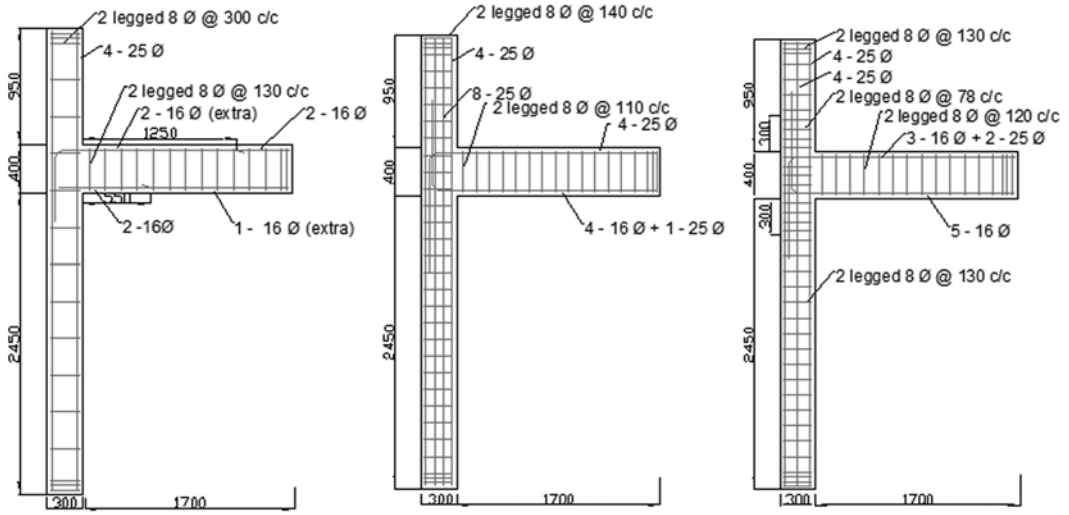

Fig. 1 Reinforcement details of the specimens considered in the present study

behaviour of RC structures or sub-assemblages using numerical studies, but the studies on the behaviour under cyclic loading are clearly inadequate. Hence, a detailed study has been carried out on the performance of the beam-column sub-assemblages under cyclic loading. In the present study, the poorly designed 'GLD' beam-column sub-assemblage (hereinafter called as SP-1) as well as 'NonDuctile' specimens designed based on Indian Standard (IS456-2000) and Eurocode (Eurocode 2 and Eurocode 8) (hereinafter called as SP-3 and SP-4, respectively) have been considered for numerical analysis. As it has been found that the 'GLD' beam-column sub-assemblages based on Indian Standard and Eurocode are quite similar, only one (based on Indian Standard) 'GLD' sub-assemblage has been considered in this study. The geometric and reinforcement details of the sub-assemblages are shown in Fig. 1. Grades of concrete and steel for the specimens have been taken as 30 MPa and 500 MPa, respectively. It is understandable that the GLD structures (representing pre-1970s) with so high strength of steel may not be feasible, but to bring uniformity among the test specimens, such strength has been chosen and designed accordingly. All sub-assemblages have the same general and cross-sectional dimensions: height of column is 3800mm and length of beam is 1700 mm with cross-sections of (300×300)mm and (300×400)mm, respectively. Table 1 presents the results obtained from the analysis of a 4-bay 3-storied RC building under dead load (DL), live load (LL) and seismic load (SL), and the load combinations according to the codal provisions. Finally, the geometry of the components (top and bottom portion of column and beam length from joint face) was chosen, as presented in Table 1, to match the bending moment distribution at the joint for which it was designed. The reinforcement details of the specimens are also presented in Table 2. Here, SP-5 and SP-6, which represent the specimens with seismic detailing, would point out the missing reinforcement of 'NonDuctile' specimens. Beam and column stirrup spacings are tabulated for joint and required adjacent zones for the confinement, then followed by the rest part of the member respectively. Further details on the experimental studies on those specimens under reverse cyclic load can be seen elsewhere (Novák *et al*. 2008).

Since, the behaviour of beam-column sub-assemblages with different variables can not be fully studied through experimental investigations, validated numerical models are also required for further studies on behaviour of beam-column sub-assemblage with different variables which would pave the way for achieving the better and optimally designed structures. In the present study, a non-linear FE program ATENA which is exclusively formulated for reinforced concrete structures has been used. In this paper, first, material properties chosen, geometric modelling adopted and analysis parameters considered have been discussed in brief and it is followed by the results and discussion on numerical studies of the 'GLD' and 'NonDuctile' sub-assemblages and further parametric studies.

2. Material properties

In any numerical investigation, it is utmost important to provide the material properties as realistic as possible. Like any other Finite Element analysis, in ATENA also certain assumptions and suitable theoretical simplifications are made. For understanding the assumptions in- and applicability of-ATENA for non-linear analysis of reinforced concrete structures/components, a highlight on necessary issues concerning the material models and their behaviour used in ATENA (2006) is presented in brief.

Table 1. Calculations for arriving at the geometry of the specimens (in kN, m)

Load combinations	Bottom column moment at joint (M_b)	Top column moment at joint (M_b)	Axial load at bottom of bottom column (p_1)	Axial load at bottom of top column (p_2)	p_1-p_2	Beam moment at the joint (Mu)	Length of column below joint =Stores height*(M_b)/(M_b+M_t)	Length of column above joint =Stores height*(M_t)/(M_b+M_t)	Length of beam Mu/(p_1-p_2)
1.5DL+1.5SL (Indian standard)	202	75.69	25.35	104.7	151.65	274.9	2.546	0.954	1.8126
1.2DL+1.2LL+1.2SL (Indian standard)	176.83	78.65	285	122.64	162.36	253.2	2.42252	1.07748	1.5596
1.0DL+0.6LL+1.0SL (Eurocode)	142.28	59.51	210.86	89.24	121.62	199.9	2.4678	1.03219	1.64373
Average							2.479	1.02	1.672
Adopted for specimens							2.5	1.0	1.7

Table 2. Specimens details

Specimens	Code of practice	Reinforcement details			
		Beam main	Column main	Beam stirrup	Column stirrup
Specimen-1 (**SP-1**) GLD	IS 456-2000	(2+2*)-16∅ top (2+1*)-16∅ bot (* =extra reinf)	4-25∅	2^L -8∅ @130 c/c	2^L -8∅@300 c/c
Specimen-3 (**SP-3**) GLD+Seismic load	IS 456-2000	4-25∅ top 4-16∅+1-25∅ bot	12-25∅	2^L -8∅ @110 c/c	2^L -8∅@140 c/c
Specimen-5 (**SP-5**)* GLD+Seismic load+ductile detailing	IS 456-2000, IS 13920-1998	4-25∅ top 4-16∅+1-25∅ bot	12-25∅	2^L -10∅ @100 /120 c/c	2^L -10∅@75/150 c/c
Specimen-4 (**SP-4**) GLD+Seismic load	EC 2: 1-1:2004, EN 1990:2002 EC 8 (EN 1998-1:2004)	3-16∅+2-25∅ top 5-16∅ bot	8-25∅	2^L -8∅ @120 c/c	2^L -8∅@130 c/c
Specimen-6 (**SP-6**)* GLD+Seismic load+ductile detailing (medium)	EC 2: 1-1:2004, EN 1990:2002 EC 8 (EN 1998-1:2004)	5-20∅ top 3-20∅ bot	8-25∅	2^L -10∅ @100/150 c/c	2^L -10∅@120/200 c/c

*Results obtained from the ductile specimens SP-5 and SP-6 are not presented in the present study. Here, reinforcement details of the ductile specimens are presented to show the missing ductile details of the 'NonDuctile' specimens

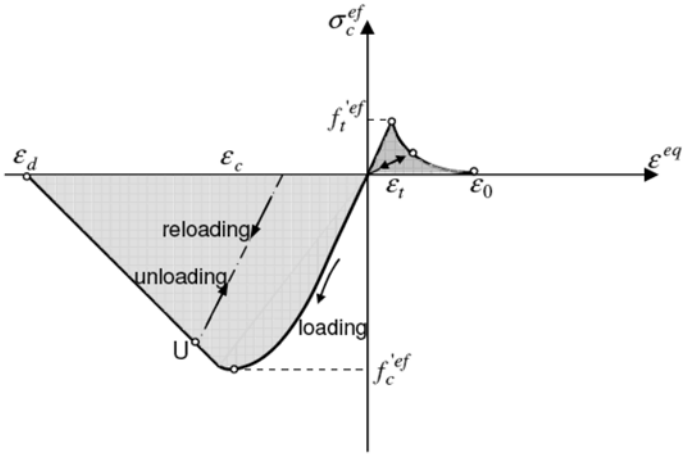

Fig. 2 Uniaxial constitutive law for concrete

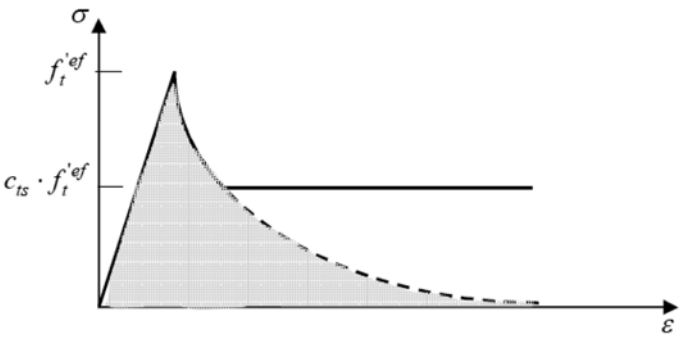

Fig. 3 Tension stiffening

2.1 Concrete

Concrete model in ATENA is based on plane stress constitutive model. A smeared approach is used to model the crack properties so that the material properties defined for a material point are valid within a certain material volume. Material model for concrete in ATENA has been included with the following effects of the concrete behaviour: (i) Non-linear behaviour of concrete in compression including hardening and softening, (ii) Fracture of concrete in tension based on non-linear fracture mechanics, (iii) Biaxial strength failure criterion, (iv) Reduction of compressive strength after cracking, (v)Tension stiffening effect, (vi) Reduction in shear stiffness after cracking (variable shear retention), and (vii) Fixed and rotating crack model based on crack direction.

It is important to mention here that actually measured average cube strength of concrete obtained from the test was 36.17 MPa. The complete equivalent uniaxial stress-strain diagram for concrete is shown in Fig. 2. Generally, unloading is assumed to be a straight line parallel to the initial stiffness of concrete, and with subsequent reloading, linear unloading path is followed until the last loading point U is reached. After this point, the loading function is resumed (as shown in the above figure). It is to state that the global hysteresis is mainly caused by the effects, such as (i) hysteresis of concrete, (ii) opening/development and closing of new cracks, (iii) hysteresis of the reinforcement,

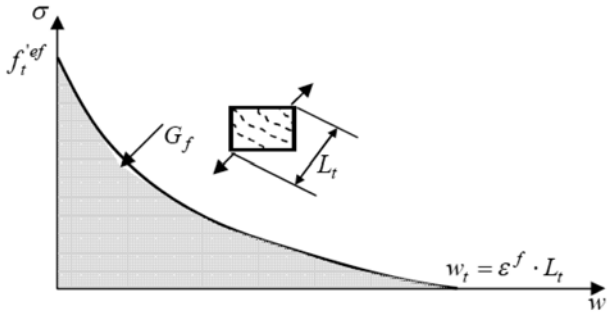

Fig. 4 Softening displacement and corresponding stress-strain diagram in compression

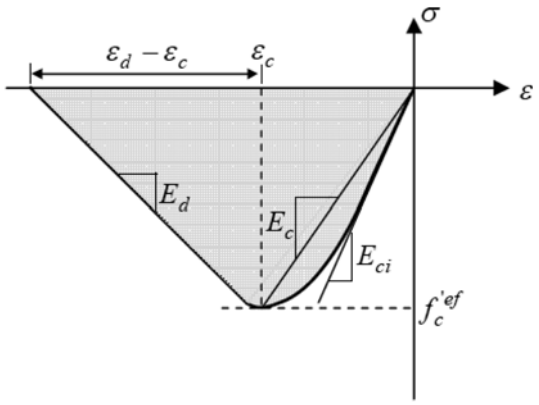

Fig. 5 Tensile softening and characteristic length

(iv) bond failure and slip between concrete and reinforcement, and (v) shear on cracks. Though concrete model "Cementitius2" in ATENA does not include any hysteresis behaviour, other parameters are effectively incorporated in the concrete model used in the present study. It is important to mention that tension stiffening which represents the relative limiting value of tensile strength of concrete (as shown in Fig. 3) was considered as 0.4. The crack opening w is computed from the summation of fracturing strain and the current increment of fracturing strain. Finally, the total sum of fracturing strain is multiplied by characteristic length L_t. Bazant and Oh (1983) proposed the characteristic length as a crack band size. In ATENA, crack band size L_t is calculated as a size of the element projection in the crack direction (as shown in Fig. 4). Further, in ATENA, the descending branch of the compressive stress-strain behaviour of concrete (as shown in Fig. 5) is defined by $w_{d,max}$. It is the maximum possible post peak displacement of defined concrete. From the experiments of Van Mier (1986) the value of $w_{d,max}$=0.5 mm was proposed for normal concrete. But, this value leads to brittle failure of concrete in the corner of beam-column joint under multi-axial compression. Further, it was shown by Van Mier that behaviour of concrete under multi-axial compression is much more ductile than under uniaxial tests. It is found from the present study on numerical analysis of exterior sub-assemblages that a value of 5 mm would provide an appreciable result. This value is used in the present study as default for the definition of the softening in compression.

In the present plasticity model of concrete, Menétrey-Willam's (1995) three parameter failure surface as given in Eq. (1) is used in the ATENA material model

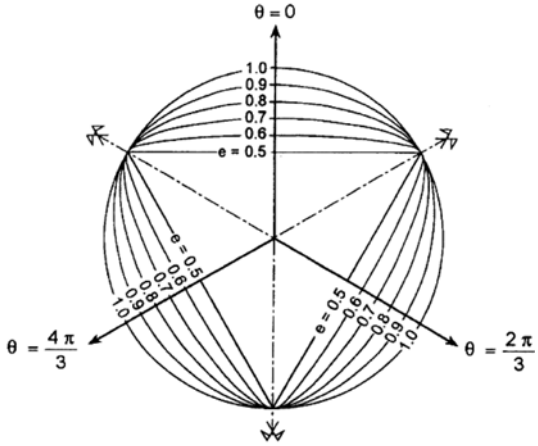

Fig. 6 Failure surfaces with different e

$$F^p(\xi_{m-w},\rho_{m-w},\theta_{m-w}) = \left[\sqrt{1.5}\frac{\rho_{m-w}}{f_c'}\right]^2 + m(f_c', f_t', e)\left[\frac{\rho_{m-w}}{\sqrt{6}f_c'}r(\theta_{m-w},e) + \frac{\xi_{m-w}}{\sqrt{3}f_c'}\right] - c = 0 \quad (1)$$

Where, ξ_{m-w}, ρ_{m-w} and θ_{m-w} are hydrostatic length, deviatoric length and angle of the stress vector in Haigh-Westergaard stress space. $r(\theta_{m-w},e)$ is an elliptical function, f_c' is compressive strength of concrete, f_t' is tensile strength of concrete, hardening/softening is controlled by the parameter c, and e is the roundness of the failure surface (between 0.5 to 1 where 0.5 and 1 represent the failure surface with sharp corners and fully circular around the hydrostatic surface, respectively as shown in Fig. 6. The position of failure surfaces can move depending on the value of strain hardening/softening parameter.

Remmel (1994) presented an approach to calculate the fracture energy as given in Eq. (2) where compressive strength of concrete and particle size were the parameters. Here, the empirical factor was taken as 65 for particle size of 16 mm. Results obtained from a series of tests were compared by Remmel with Eq. (2) and the equation proposed in CEB-FIP Model Code 90 (1990). It was pointed out that there was a good agreement among the results obtained from the tests and the equation proposed by Remmel whereas CEB-FIP Model Code 90 provides almost 25% lesser value than that obtained from the tests. In the present study, fracture energy was calculated as proposed by Remmel.

$$G_F = 65 \cdot \ln\left(1 + \frac{f_c}{10}\right) \text{ [N/m]} \quad (2)$$

2.2 Reinforcement

In FE model, the reinforcements (both longitudinal and transverse) were modelled as discrete reinforcing bars in form of truss elements. All sizes of reinforcement bars that were used in the experiments were tested to evaluate the stress-strain behaviour. Actually measured average yield strength of reinforcement bars obtained from the rebar tensile test was 533 MPa. Based on the behaviour found from material test, reinforcement bars in the numerical models were assumed to

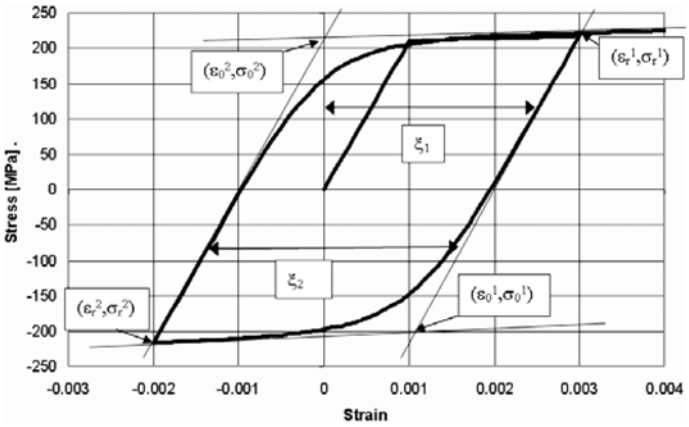

Fig. 7 Cycling reinforcement model based on Menegotto and Pinto (1973)

follow the bilinear law, i.e., elastic-plastic behaviour with strain hardening. It is also important to note that the behaviour of different diameters of reinforcements showed a variation in stress-strain relations though the elastic part was quite similar. Hence, in the numerical models post-yield behaviour of reinforcement bars with different diameters was incorporated accordingly. In ATENA, Bauschinger's effect for reinforcement under cyclic loading is incorporated (as shown in Fig. 7) by using Menegotto-Pinto model (1973).

2.3 Reinforcement bond model

Bond-slip relationship for reinforcement bars was chosen as proposed by CEB-FIB model code 90 (1990) as shown in Fig. 8. Concrete was considered to be without any confinement and the quality of construction was assumed to be poor. Bond strength has been calculated at different level of slips whereas different levels of slip depend on bond condition and degree of confinement in concrete. In the present study no special cyclic bond-slip has been used. It has been found from the preliminary analysis that by using sufficiently small elements and cycling model for the reinforcement, role of

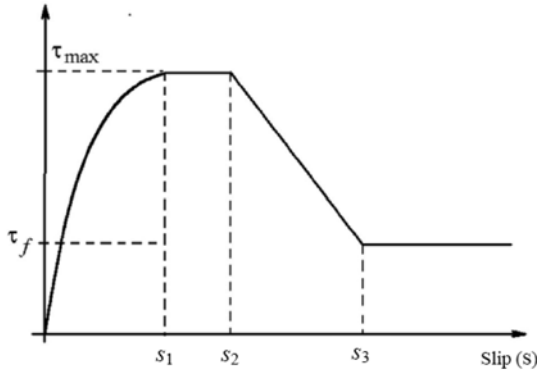

Fig. 8 Bond-slip relationship proposed by CEB-FIP model code 1990

bond model under cyclic loading can be minimised and the analysis can be able to capture by the cracking of surrounding concrete elements efficiently.

3. Geometric modelling

Different micro-elements were created for different parts of the specimens based on D-region and B-regions. Model corresponding to the geometry and the reinforcement of the poorly designed 'GLD' sub-assemblage is shown in Fig. 9. Concrete parts of the models were modelled using quadratic "Brick"- and steel plates (at load/reaction zones) were modelled using "Tetrahedral"- solid elements. Since, these numerical analyses were computational intensive due to cyclic loading, two different sizes of FE mesh were used. In the joint zone, three adjacent macro-elements were meshed with 50 mm size and the rest part of the model was meshed with 100 mm. Generated finite element mesh of the typical numerical model for the specimens is shown in Fig. 9. During experiment, specimens were provided with column top and bottom

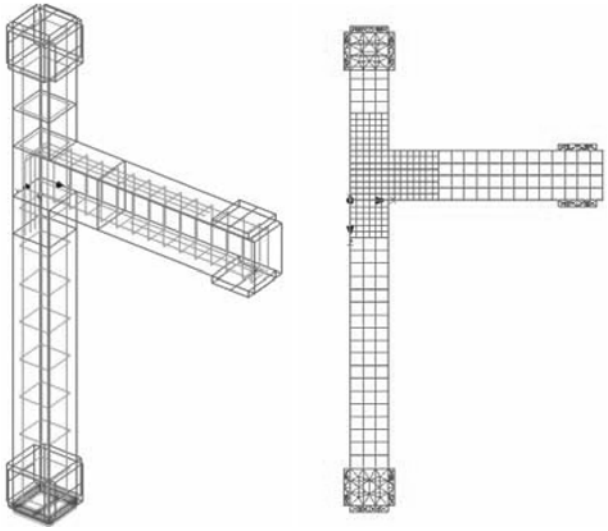

Fig. 9 Geometry and mesh distribution of the numerical model

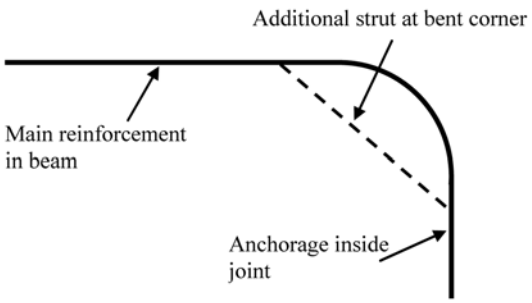

Fig. 10 Modelling of reinforcement at bent locations

hinges using steel plates and rollers. These steel plates with rollers were inserted in between specimen and steel channels. It is obvious that during loading in beam tip, there was a movement at column top and bottom depending on the stiffness of the steel channel which held the specimen and the hinging arrangement. To simulate this behaviour, springs were modelled at outer and inner sides of top and bottom ends of the column which would provide a certain degree of flexibility at the support locations. It is also to mention that the springs in the numerical models were effective in compression only. Here, reinforcements were modelled as discrete truss elements inside concrete. Curvature of beam bending reinforcement inside joint was modelled as truss members in polygons. It is significant to mention here that since the reinforcements were truss elements, effect of anchorage could not be simulated by mere modelling of the bent of reinforcement in one-dimensional form. Hence, another strut with same element property was provided at the bent corner of reinforcement which would make the reinforcement a two-dimensional truss (as shown in Fig. 10). Bond-slip relationship was incorporated in each of the bending reinforcements as specified by CEB-FIP Model Code whereas the stirrups for beam and column were assumed to be perfectly bonded.

4. Analysis procedure

At first, total axial load of 300 kN in column was gradually applied in the numerical models in few steps and subsequently, the displacement cycles were applied at beam tip. Axial loading phase of the simulated model was solved by arc-length method and then the solver was changed to Newton-Raphson method during displacement cycles. For better numerical accuracy, displacements were incorporated in small steps. Initially, a convergence study was carried out with different displacement steps and finally, a displacement increment of 1 mm in each step was chosen by maintaining the accuracy of results and total number of steps required to simulate the experimental investigations of the specimens subjected to cyclic loading. Despite the limitation of the concrete model "Cementitius2" as stated in section 2.1, only one cycle at each displacement level was adopted in the present study because it was observed that analyzing the entire

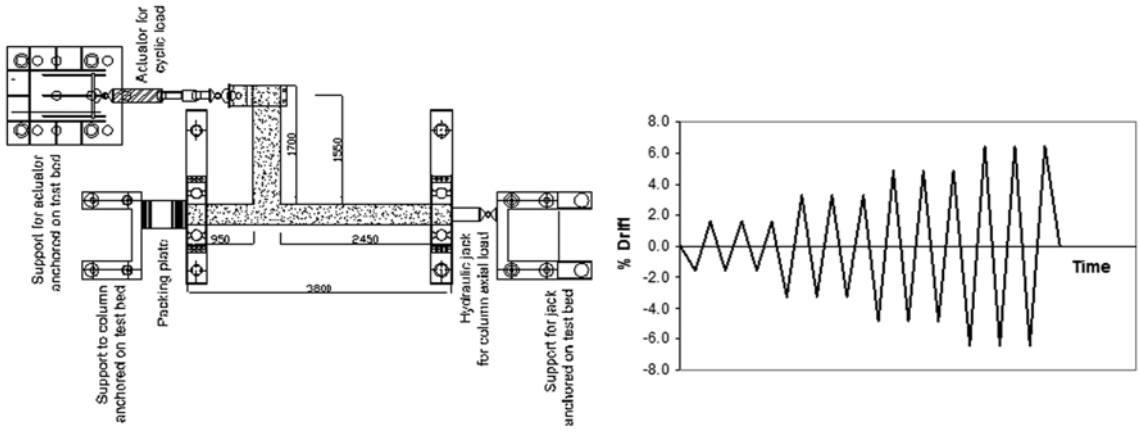

Fig. 11 Schematic diagram of the test set up placed on test floor and load history

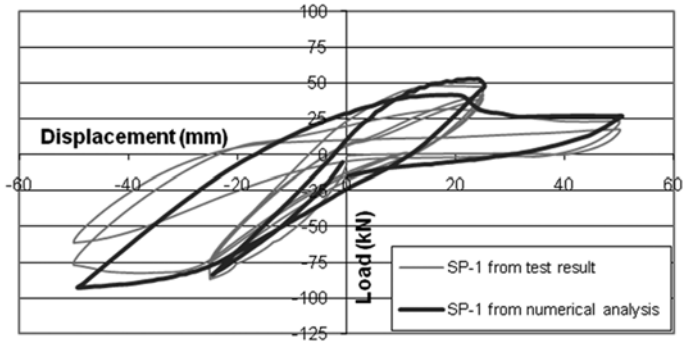

Fig. 12 Load-displacement hysteresis for SP-1 from test and numerical analysis

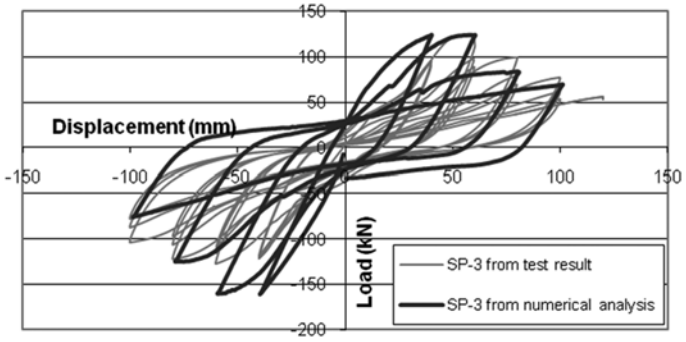

Fig. 13 Load-displacement hysteresis for SP-3 from test and numerical analysis

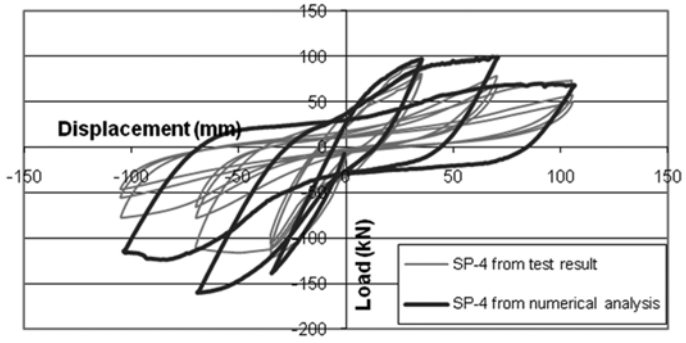

Fig. 14 Load-displacement hysteresis for SP-4 from test and numerical analysis

displacement history (3 repeated cycles at each displacement level used during the test as shown in Fig. 11) with adequately small increments (1 mm) of displacement in numerical analysis demands enormous computational time and space. A detailed discussion on results obtained from numerical analysis under repetitive and non-repetitive loading can be found elsewhere (Sasmal 2009).

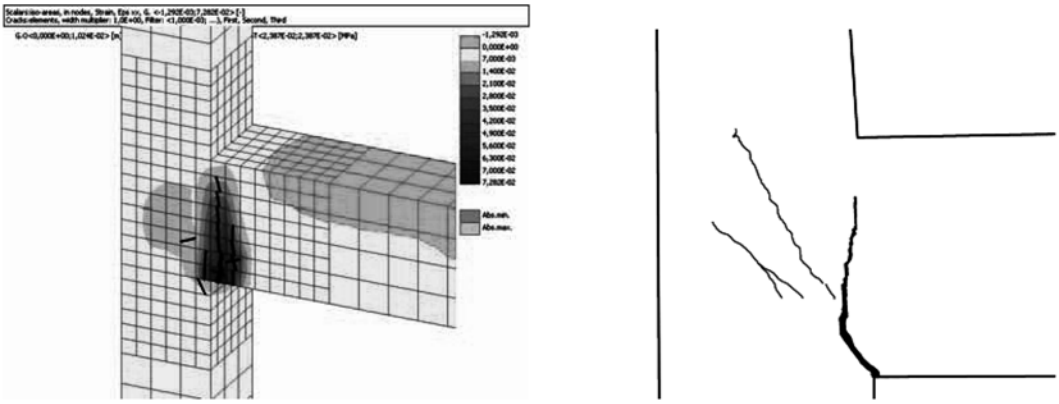

Fig. 15 Comparison of crack pattern for SP-1 from numerical analysis and test

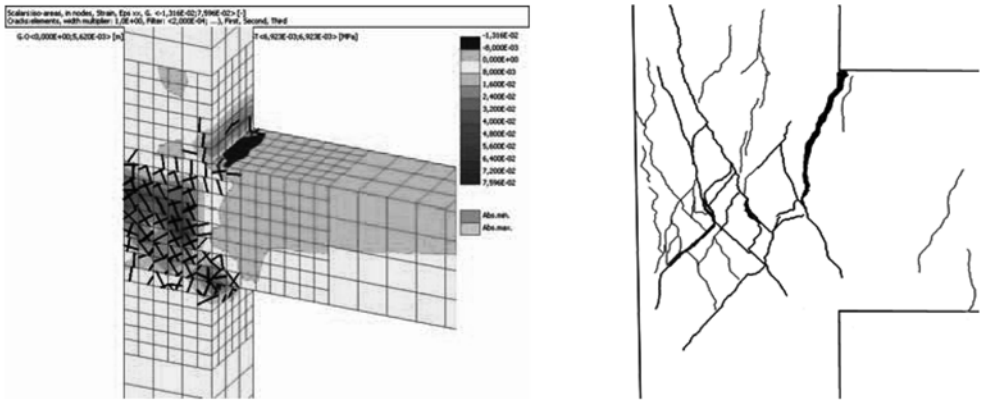

Fig. 16 Comparison of crack pattern for SP-3 from numerical analysis and test

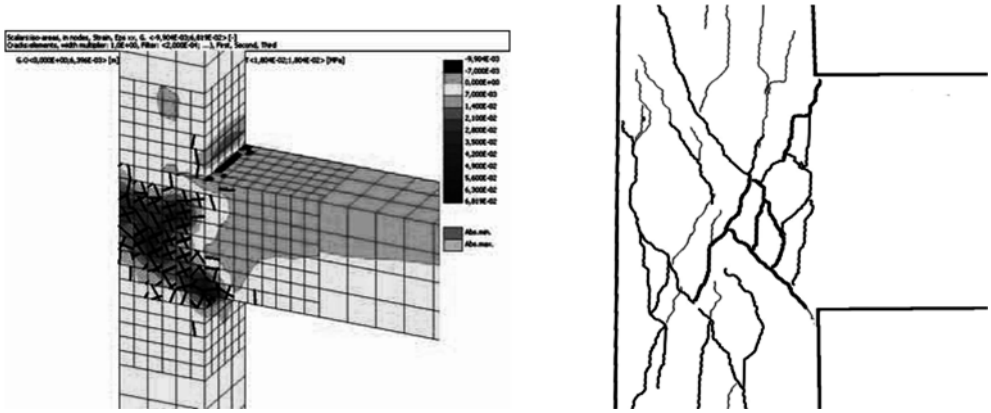

Fig. 17 Comparison of crack pattern for SP-4 from numerical analysis and test

5. Results and discussion

The load-displacement hysteresis of 'GLD' sub-assemblage (SP-1) and 'NonDuctile' beam-column sub-assemblages (SP-3 and SP-4) obtained from the numerical analysis and the test is shown in Figs. 12-14. The figures (Fig. 12 to Fig. 14) show that the results obtained from the numerical analysis are well corroborated with that of experimental results. Along with the load-displacement hysteresis, it is also important to know the damage pattern of the specimens determined from the numerical analysis. The final damage patterns of the 'GLD' and the 'NonDuctile' sub-assemblages obtained from the numerical analysis and that observed during experiment are shown in Fig. 15 to Fig. 17, respectively. Crack patterns from the numerical analysis showed that the final damage in 'GLD' specimen was due to failure of bond in beam bottom reinforcement which is well supported by the experimental observations. Further, the joint failure of SP-3 and SP-4 obtained from the numerical analyses are identical to that observed during experiment. Further, both experimental investigation and numerical analysis confirmed that there was no damage in column region of any of the sub-assemblages. It is evident from the figures that along with the load-displacement hysteresis, the numerical analysis can predict the crack pattern and final damage scenario quite accurately.

6. Parametric studies from numerical analysis

After obtaining the validated FE models for 'GLD' and 'NonDuctile' sub-assemblages, it was attempted to explore other critical parameters.

6.1 Correlation of energy dissipation

Since in experimental investigation three repeated cycles were applied at each displacement level whereas the numerical models were validated for single cycle at each displacement level, it is of great use to correlate the energy dissipations obtained from the test and numerical analysis so that the results obtained from the numerical analysis can provide a range in energy dissipation during real test. Towards this, all the experimented sub-assemblages (discussion on other sub-assemblages with different types of detailing is not presented as it is out of the scope of the study) were

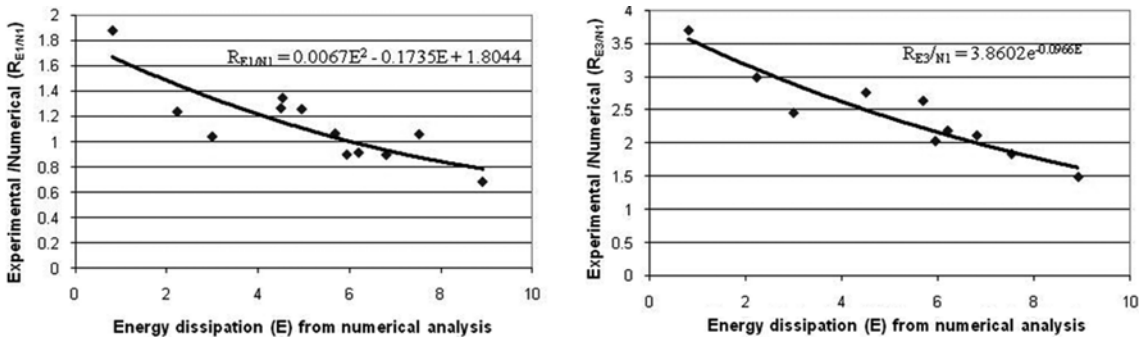

Fig. 18 Single cycle- and total-energy dissipation from experimental and numerical study

numerically analysed. Energy dissipation in first cycle from experiment (E1) and that of numerical analysis (N1) and energy dissipation in all three cycles from experiment (E3) and single cycle from numerical analysis (N1) are shown in Fig. 18. Here, energy dissipation was calculated in kNm. The study and proposed relations between energy dissipation obtained from experimental- and numerical-investigation (shown in the figures) would help in practice to provide the guideline in evaluating the actual energy dissipation of any exterior sub-assemblage by obtaining that from numerical analysis. This would facilitate in improving the design and detailing of the sub-assemblage before adopting for a seismic resistant structure since the experimental investigations are not always possible, time consuming and costly as well.

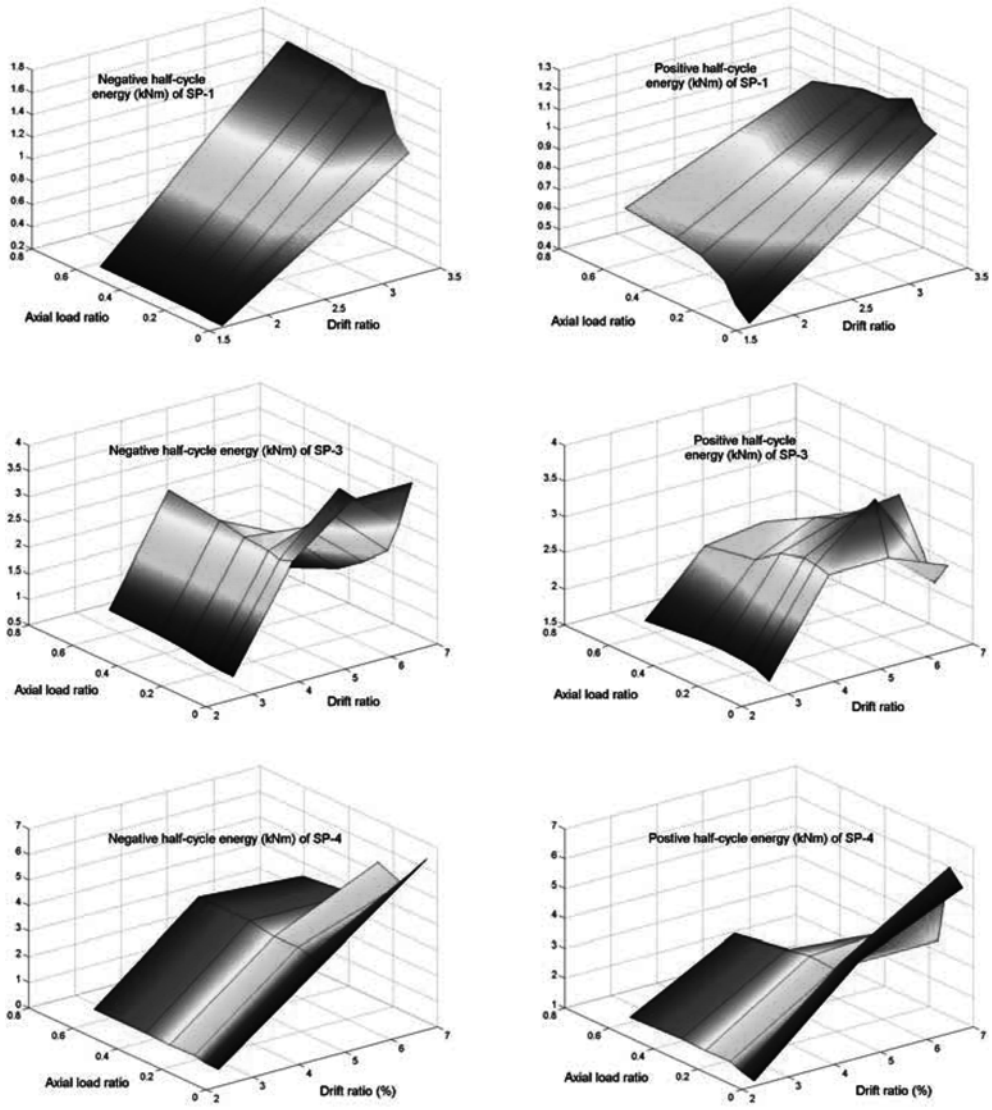

Fig. 19 Energy dissipation (kNm) of the specimens with variation of axial load and drift ratio

6.2 Axial load effect

One of the most interesting issues still being discussed is the effect of axial load on seismic performance of RC sub-assemblages and structures as a whole. Several researchers have reported inconsistent results and observations on the performance of RC structure where axial compression loading was a parameter. For example, Paulay *et al*. (1978) and Ghee *et al*. (1989) reported that increase in axial load in column would improve the shear strength of the section. Priestley and Park (1987) brought out the enhancement of moment carrying capacity at any section due to axial load effect. On the other hand, Lim and McLean (1991) suggested that higher axial load produced

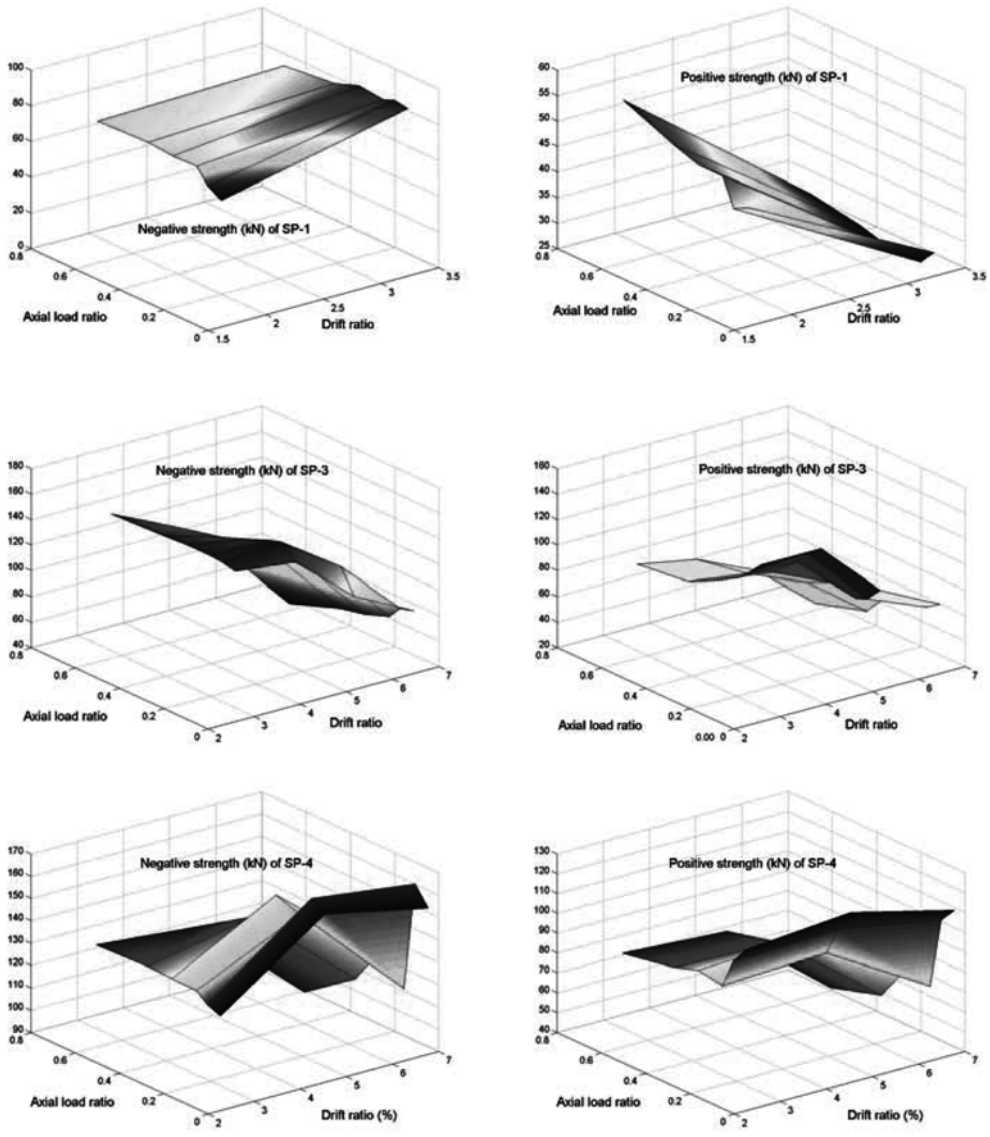

Fig. 20 Strength (kN) of the specimens with variation of axial load and drift ratio

greater drop in strength whereas Mo and Nien (2002) observed that a greater axial load produced higher maximum load. It is reported by Au and Bai (2006) that the moment capacity tends to increase with compressive axial load when axial load is less that 40-50% of the capacity beyond which the moment capacity drops. It was further noticed that with increasing axial load, the flexural ductility factor always decreases. Li *et al*. (2009) brought out the beneficial effect of column axial load (compressive) on joint shear resistance and bond strength, and detrimental effect on bond deterioration. But, it is almost agreed by most of the researchers that ductility of any section deteriorates as the level of axial load increases. In view of this, it is important to know the behaviour of sub-assemblages considered in this study under varying axial load. Using the validated FE models for 'GLD' and 'NonDuctile' specimens, parameters like rate of strength degradation and change in energy dissipation in every positive and negative cycle have been studied under a wide range of axial load ratios (defined as axial load in column divided by column axial capacity) and different drift ratios. Energy dissipation and the strength of the specimens (SP-1, SP-3 and SP-4) during cyclic loading are shown in Fig. 19 and Fig. 20, respectively, where drift ratio and axial load ratios are the parameters.

From the study (as shown in Fig. 19 and Fig. 20) on the axial load effect, a number of important observations have been made. (i) During negative loading (downward) with low drift ratio, axial load has negligible impact on energy dissipation of 'GLD' specimens whereas axial load provides a positive influence on negative energy dissipation under higher drift ratios. (ii) Unlike negative loading, during positive (upward) loading on 'GLD' specimen, axial load plays an important role in increasing energy dissipation under lower drift ratio and this effect reduces with increase in drift ratio. (iii) Both the 'NonDuctile' specimens show a clear behaviour that with increase in axial load, energy dissipation (positive and negative) increases. But, under a high drift ratio with high axial load, the specimens become so brittle that energy dissipation suddenly drops. Reduction in energy dissipation with higher axial load and higher drift ratio is more in Eurocode based 'NonDuctile' specimen in comparison to the Indian Standard based specimen. (iv) Strength corresponding to negative load in specimens increases with increase in axial load when drift ratio is not high. Under high drift ratio, though the decrease in negative strength is not so prominent in 'GLD' specimens, but in 'NonDuctile' specimens it is drastic. (v) Similar behaviour has been noted during change in strength under positive displacement, i.e., in low drift ratio axial load in column brings a favourable effect in change of positive strength of specimens though it does not hold good under high drifts. Moreover, presence of high axial load in column reduces its strength. From these observations on 'GLD' and 'NonDuctile' specimens, it can be stated that the inconsistent results reported by previous researchers were valid in their range of experiments where a certain range of axial load and drift ratio on particular specimen(s) were considered. So, finally it is noteworthy to mention that an increase in axial load in column will provide a better seismic response for the structures under low seismic demand. Hence, any existing under-designed structure (both 'GLD' and 'NonDuctile') in low seismic zones may be improved or strengthened by increasing its column axial load using mechanical means such as external prestressing etc. On the other hand, in areas with high seismic demand, it will not only be invalid and insufficient, but could bring adverse effect due to increase in brittleness in the member with increase in axial load.

7. Conclusions

In the present study, the non-linear Finite Element (FE) program ATENA which is exclusively formulated for analysis of reinforced concrete structures/components has been employed for analysing (under cyclic loading) the 'GLD' and 'Nonductile' beam-column sub-assemblages representing the existing structures before the introduction of the concept of capacity design and ductile detailing. The numerical analysis of the sub-assemblages was performed using the proper geometric- and material- modelling. During these studies, computational aspects were suitably taken care of. It has been found that the results, in terms of load-displacement hysteresis and damage pattern, obtained from the numerical analysis are in close agreement with that obtained from the experimental investigations. The study shows that the appropriate and judicious use of material models and numerical analysis procedure can be able to predict a considerably close response and damage pattern of the sub-assemblages as that was obtained from the experimental studies. Further, it was attempted to correlate the energy dissipation obtained from the numerical analysis with the experimental response. The proposed relations would certainly help the practicing engineers to obtain the guideline on the performance of any proposed beam-column sub-assemblage for seismic loading and can provide a scope for further improvement in the detailing of the sub-assemblage. Axial load effect on the seismic performance of the sub-assemblages, in terms of energy dissipation and strength degradation, was also numerically investigated. It is worthy to state that further numerical studies are being carried out, based on the validated numerical models, with different material models, reinforcement detailing towards finding out adequate, feasible and optimum design rules and detailing provisions for critical regions of new RC structures.

Acknowledgements

The authors wish to express their gratitude and sincere appreciation to the director and officials of Structural Engineering Research Centre (SERC), CSIR, Chennai, India for facilitating the experimental works.

References

American Concrete Institute Committee ACI318-02, "Building Code Requirements for Reinforced Concrete (ACI 318-02)", ACI 318-95, 99, 02, Detroit, Michigan, 1995, 1999, ATENA theory manual. ATENA Program Documentation - Part 1: Theory. Revision 09/2006, Cervenka Consulting, Predvoje 22, Czech Republic, 207.

Au, F.T.K. and Bai, Z.Z (2006), "Effect of axial load on flexural behaviour of cyclically loaded RC columns", *Comput. Concrete,* **3**(4), 261-284.

Bazant, Z.P. and Oh, B.H. (1983), "Crack band theory for fracture of concrete", *Mater. Struct. RILEM*, **16**(93), 155-177.

CEN Technical Committee 250 (2005), *Eurocode 2: design of concrete structures-Part:1-1: general rules and rules for buildings*, (EN 1992-1-1:2004), CEN, Berlin, Germany, 248.

CEN Technical Committee 250/SC8 (2006), *Eurocode 8: design of structures for earthquake resistance-Part: 1: general rules, seismic actions and rules for buildings*, (ENV 1998-1:2004), CEN, Berlin, Germany, 192.

Comite Euro-International du Beton (CEB) (1990), CEB Model Code 90, Bull, d'information, No. 203, Paris, France.

Fischinger, M., Isakovic, T. and Kante, P. (2004), "Implementation of a macro model to predict seismic response

of RC structural walls", *Comput. Concrete*, **1**(2), 211-226.
Ghee, A.B., Priestley, M.J.N. and Paulay, T. (1989), "Seismic shear strength of circular reinforced concrete columns", *ACI Struct. J.*, **86**(1), 45-59.
Hegger, J., Sherif, A. and Roeser, W. (2003), "Nonseismic design of beam-column joints", *ACI Struct. J.*, **100**(5), 654-664.
Hegger, J., Sherif, A. and Roeser, W. (2004), "Nonlinear finite element analysis of reinforced concrete beam-column connections", *ACI Struct. J.*, **101**(5), 604-614.
Indian Standard (IS 456-2000) (2000), *Plain and reinforced concrete - code of practice*, Bureau of Indian Standards, New Delhi.
Li, B., Wu, Y. and Pan, T.C. (2003), "Seismic behavior of nonseismically detailed Interior beam-wide column joints-Part II: theoretical comparisons and analytical studies", *ACI Struct. J*, **100**(1), 56-65.
Li, B., Pan, T.C. and Tran, C.T.N. (2009), "Effects of axial compression load and eccentricity on seismic behavior of nonseismically detailed interior beam-wide column joints", *J. Struct. Eng. - ASCE*, **135**(7), 774-784.
Lim, K.Y. and McLean, D.I. (1991), "Scale model studies of moment-reducing hinge details in bridge columns", *ACI Struct. J.*, **88**(4), 465-474.
Marefat, M.S., Kanmohammadi, M., Bahrani, M.K. and Goli, A. (2005), "Cyclic load testing and numerical modelling of concrete columns with sub-standard seismic details", *Comput. Concrete*, **2**(5), 367-380.
Menegotto, M. and Pinto, P.E. (1973), "Method of analysis of cyclically loaded RC plane frames including changes in geometry and non-elastic behaviour of elements under combined normal force and bending." *Proc. IABSE Symposium on Resistance and Ultimate Deformability of Structures Acted on by Well Defined Repeated Loads*, 15-22.
Menétrey, P. and Willam, K.J. (1995), "Triaxial failure criterion for concrete and its generalization", *ACI Struct. J.*, **92**(3), 311-318.
Mo, Y.L. and Nien, I.C. (2002), "Seismic performance of hollow high-strength concrete bridge columns", *J. Bridge Eng. - ASCE*, **7**(6), 338-349.
Novák, B., Ramanjaneyulu, K., Roehm, C. and Sasmal, S. (2008), "Seismic performance of D-region of RC framed-structure designed according to different codal recommendations", *J. Struct. Eng.*, **35**(1), 46-51.
Pampanin, S., Christopoulos, C. and Priestley, M.J.N. (2003), "Performance-based seismic response of frame structures including residual deformations. Part II: Multi-degree of freedom systems", *J. Earthq. Eng.*, **7**(1), 119-147.
Paulay, T., Park, R. and Priestley, M.J.N. (1978), "Reinforced concrete beam-column joints under seismic actions", *ACI J. Proc.*, **75**(11), 585-593.
Priestley, M.J.N. and Park, R. (1987), "Strength and ductility of concrete bridge columns under seismic loading", *ACI Struct. J.*, **84**(1), 61-76.
Remmel, G. (1994), *Zum zug und schubtragverhalten von bauteilen aus hochfestem beton*, Deutscher Ausschuss für Stahlbeton, Beuth Verlag, Berlin, Germany, 77.
Sasmal, S. (2009), *Performance evaluation and strengthening of deficient beam-column sub-assemblages under cyclic loading*, Ph.D. Thesis, Institute for Lightweight Structures and Conceptual Design (ILEK), University of Stuttgart, Germany.
Sritharan, S., Priestley, M.J.N. and Seible, F. (2000), "Nonlinear finite element analyses of concrete bridge joint systems subjected to seismic actions", *Finite Elem. Anal. Des.*, **36**(3-4), 215-233.
Van Mier, J.G.M. (1986), "Multi-axial strain-softening of concrete, Part I: fracture", *Mater. Struct. RILEM*, **19**(111), 179-190.
Zhou, H. (2009), "Reconsideration of seismic performance and design of beam-column joints of earthquake resistant reinforced concrete frames", *J. Struct. Eng. - ASCE*, **135**(7), 762-773.

CC